

TN 277

**DNA 3885T**

# **HIGHLY SPACE CHARGE LIMITED SGEMP CALCULATIONS**

Mission Research Corporation  
735 State Street  
Santa Barbara, California 93101

June 1975

Topical Report

**CONTRACT No. DNA 001-75-C-0125**

**APPROVED FOR PUBLIC RELEASE;  
DISTRIBUTION UNLIMITED.**

THIS WORK SPONSORED BY THE DEFENSE NUCLEAR AGENCY  
UNDER RDT&E RMSS CODE B323075464 R99QAXEB06954 H2590D.

Prepared for  
Director  
**DEFENSE NUCLEAR AGENCY**  
Washington, D. C. 20305





UNCLASSIFIED

SECURITY CLASSIFICATION OF THIS PAGE (When Data Entered)

REPORT DOCUMENTATION PAGE		READ INSTRUCTIONS BEFORE COMPLETING FORM
1. REPORT NUMBER DNA 3885T	2. GOVT ACCESSION NO.	3. RECIPIENT'S CATALOG NUMBER
4. TITLE (and Subtitle) HIGHLY SPACE CHARGE LIMITED SGEMP CALCULATIONS		5. TYPE OF REPORT & PERIOD COVERED Topical Report
		6. PERFORMING ORG. REPORT NUMBER MRC-R-190
7. AUTHOR(s) Daniel F. Higgins Conrad L. Longmire		8. CONTRACT OR GRANT NUMBER(s) DNA 001-75-C-0125
		10. PROGRAM ELEMENT, PROJECT, TASK AREA & WORK UNIT NUMBERS Subtask R99QAXEBO69-54
9. PERFORMING ORGANIZATION NAME AND ADDRESS Mission Research Corporation 735 State Street Santa Barbara, California 93101		12. REPORT DATE June 1975
		13. NUMBER OF PAGES 42
11. CONTROLLING OFFICE NAME AND ADDRESS Director Defense Nuclear Agency Washington, D.C. 20305		15. SECURITY CLASS (of this report) UNCLASSIFIED
		15a. DECLASSIFICATION/DOWNGRADING SCHEDULE
14. MONITORING AGENCY NAME & ADDRESS (if different from Controlling Office)		
16. DISTRIBUTION STATEMENT (of this Report) Approved for public release; distribution unlimited.		
17. DISTRIBUTION STATEMENT (of the abstract entered in Block 20, if different from Report)		
18. SUPPLEMENTARY NOTES This work sponsored by the Defense Nuclear Agency under RDP&E RMSS Code B323075464 R99QAXEBO6954 H2590D.		
19. KEY WORDS (Continue on reverse side if necessary and identify by block number) SGEMP Space-Charge-Limiting Finite Difference Calculations Steady State Approximation		
20. ABSTRACT (Continue on reverse side if necessary and identify by block number) This report reviews and compares several calculational methods for studying the space-charge-limited SGEMP problem. Included are early-time approximations, steady-state calculations, and finite difference techniques. A boundary layer treatment using steady-state theory is also developed. The report discusses how this boundary layer treatment can be incorporated into a finite difference code in a way that subdivides the finite difference		

DD FORM 1473  
1 JAN 73

EDITION OF 1 NOV 65 IS OBSOLETE

UNCLASSIFIED

SECURITY CLASSIFICATION OF THIS PAGE (When Data Entered)

UNCLASSIFIED

SECURITY CLASSIFICATION OF THIS PAGE(When Data Entered)

20. ABSTRACT (Continued)

cells next to emission surfaces. This subdivision makes it possible to calculate highly space-charge-limited SGEMP response without requiring extremely fine mesh cells.

UNCLASSIFIED

SECURITY CLASSIFICATION OF THIS PAGE(When Data Entered)

## TABLE OF CONTENTS

	PAGE
LIST OF ILLUSTRATIONS	2
SECTION 1—INTRODUCTION	3
SECTION 2—EARLY TIME APPROXIMATIONS	4
SECTION 3—STEADY STATE APPROXIMATIONS	7
SECTION 4—FINITE DIFFERENCE CALCULATIONS	14
SECTION 5—BOUNDARY LAYER TREATMENT	17
SECTION 6—SUMMARY	21
REFERENCES	22
APPENDIX A—EARLY-TIME NON-SCREENING APPROXIMATION	23
APPENDIX B—STEADY STATE	27
APPENDIX C—RELATION BETWEEN EMISSION SPECTRUM AND PHASE SPACE DENSITY	29

## LIST OF ILLUSTRATIONS

FIGURE		PAGE
1	Time, $t_1$ , that electrons first start returning to emission surface as a function of initial velocity, $v_0$ , and peak emission current, $J$ (Equation 4).	6
2	Boundary layer thickness, $x_{\max}$ , as a function of emission current density, $J$ —steady state approximation (Equation 9).	9
3	Comparison of early time approximation, steady state approximation, and finite difference calculation of surface electric field (one-dimensional planar geometry). ( $J_{\text{peak}}$ is the peak emission current, before space charge limiting, and $t_1$ is the calculated time that electrons first start returning.)	15
4	2-D finite difference mesh.	18

## SECTION 1

### INTRODUCTION

When incident photons cause the emission of electrons from exposed surfaces, electromagnetic fields are created. In certain instances, these fields become large enough to rapidly pull back the majority of emitted electrons. This space charge limiting of the net emission current creates, in effect, a boundary layer near the emission surface. Low-energy electrons will be trapped inside this boundary layer, while higher energy electrons will escape after having lost some kinetic energy.

The effect of space charge limiting is to reduce the net emission current, thus decreasing the resulting electromagnetic fields and structural replacement currents. Accurate calculation of such fields and currents is made more difficult, however, due to the need for determining which electrons are the prime drivers for SGEMP effects. This paper will investigate several techniques for calculating SGEMP response under highly space charge limited conditions. Such techniques include early-time approximations, steady-state theory, finite difference particle tracking codes, and various boundary layer calculations.

SECTION 2  
EARLY TIME APPROXIMATIONS

A one-dimensional early-time approximation was developed by Karzas and Latter<sup>1</sup> for determining when monoenergetic electrons will begin returning to the emission surface. A non-screening approximation is made where it is assumed that each electron moves in a constant accelerating field equal to the field at the emission surface at the time of the electron's emission.

Up to the time,  $t_1$ , when the first returning electron returns to the emission surface, the electric field at the emission surface is just (MKS units)

$$E(x=0) = \frac{eY}{\epsilon_0} \int_0^t R(t') dt' , \quad (1)$$

where

$Y$  = electron yield (number of electrons emitted per unit area)

$e$  = electron charge

$\epsilon_0 = 8.854 \times 10^{-12}$  farad/m

and

$R(t)$  is the electron emission rate normalized so that

$$\int_0^{\infty} R(t') dt' = 1 . \quad (2)$$



For calculational simplicity, assume that  $R(t)$  is a simple triangular function with a risetime and full-width-at-half-maximum of time  $T$ . One can then show (see Appendix A) that for monoenergetic electrons ejected normal to the emission surface with initial velocity  $v_0$ , the first returning electrons return to the emission surface at time

$$t_1 = 3 \left[ \frac{m\epsilon_0}{e^2} \right]^{1/3} \left[ \frac{v_0 T^2}{Y} \right]^{1/3}, \quad (3)$$

where  $m$  is the electron mass.

The time  $t_1$  can also be expressed as

$$t_1 = 3 \left[ \frac{m\epsilon_0}{e} \right]^{1/3} \left[ \frac{v_0 T}{J} \right]^{1/3}, \quad (4)$$

where the peak emission current density,  $J$ , is defined by

$$J = \frac{eY}{T}. \quad (5)$$

It is interesting to note that the time  $t_1$  depends not only on the peak emission current density,  $J$ , but also on the pulse risetime,  $T$ .

Since  $t_1$  is the time that electrons first start returning, the time  $t_1$  also marks the point that the early-time non-screening approximation begins to become invalid.

Note that  $t_1$  varies as  $v_0^{1/3}$ . Since kinetic energy,  $w$ , is proportional to  $v_0^2$ , it appears that  $t_1$  is not highly sensitive to the electron energy spectrum ( $t_1 \propto w^{1/6}$ ). However,  $t_1$  is dependent on the pulse time history ( $t_1 \propto T^{2/3}$ ) and the total electron yield ( $t_1 \propto Y^{-1/3}$ ).

Calculation of  $t_1$  gives a useful estimate of just how long it takes for space charge limiting effects to become important. Figure 1 shows some typical values of  $t_1$  as a function of initial electron velocity and peak current density. (Note that Equations 3 and 5 are valid only if  $t_1 \leq T$ .)

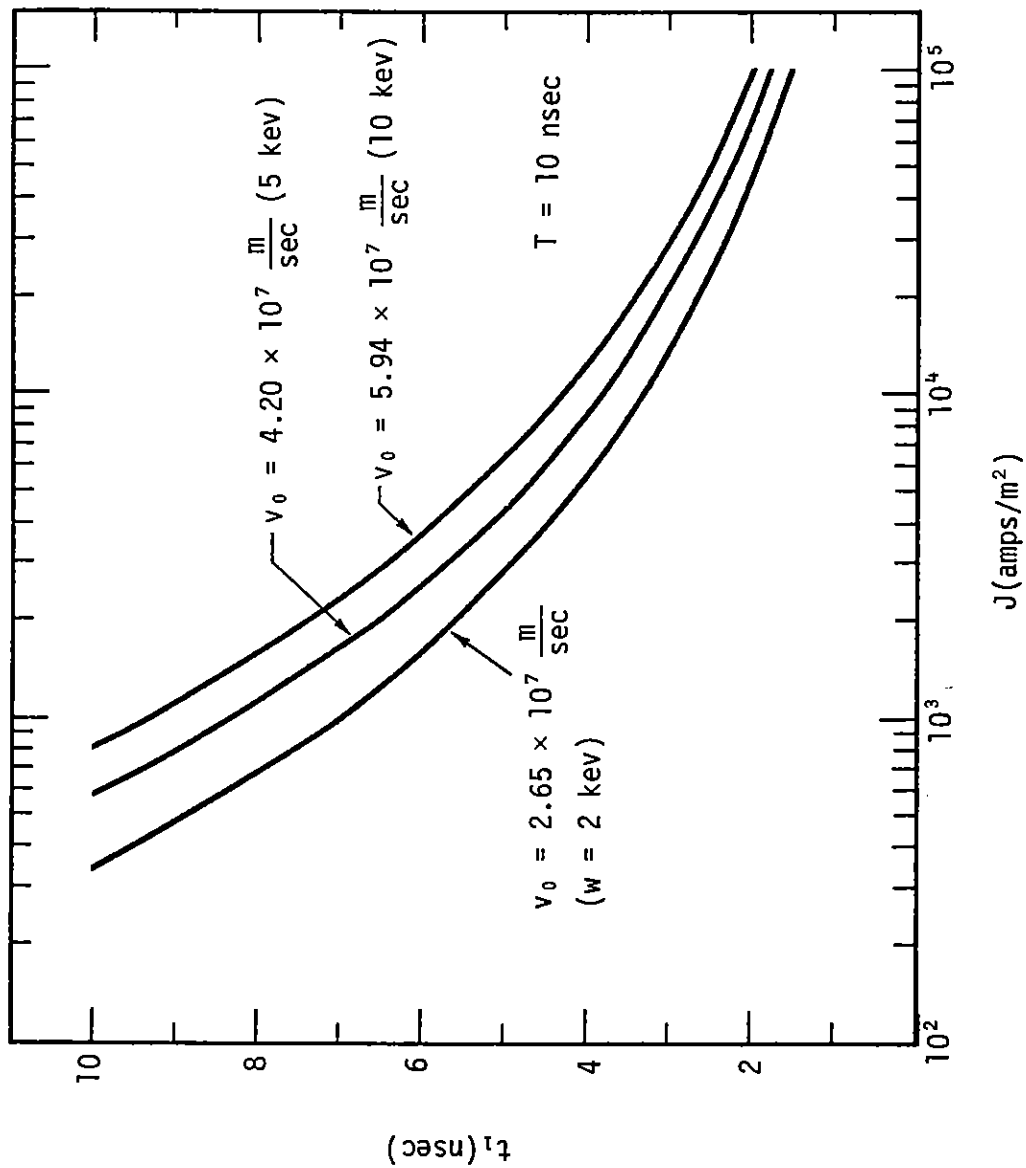


Figure 1. Time,  $t_1$ , that electrons first start returning to emission surface as a function of initial velocity,  $v_0$ , and peak emission current,  $J$  (Equation 4).

SECTION 3  
STEADY STATE APPROXIMATIONS

Steady-state calculations assume electrons are being emitted at the same rate they are returning to the emission surface. Such approximations are accurate as long as electron transit times (time between emission and return) are short compared to any other times of interest. Karzas and Latter<sup>1</sup>, Hale<sup>2</sup>, and others have investigated the steady-state problem by solving Poisson's equation for various initial velocity distributions.

For a monoenergetic electron source, the electron transit time is found to be (see Appendix B)

$$\tau_t = 2 \left[ \frac{v_0}{A} \right]^{1/2}, \quad (6)$$

where

$$A = \frac{e^2 Y R(t)}{m \epsilon_0}, \quad (7)$$

and the variables have the same definition as in Section 2. Note that A can also be written as

$$A = \frac{e J(t)}{m \epsilon_0}. \quad (8)$$

where  $J(t) \equiv e Y R(t)$  is the current density of emitted electrons at the emission surface at time  $t$ .

Using the same approximations, the maximum distance an electron moves,  $x_{\max}$ , is given by

$$x_{\max} = \frac{v_0^{3/2}}{3\sqrt{A}} . \quad (9)$$

This simple steady-state approximation can thus be used to estimate the thickness of any "boundary layer" formed by space charge limiting. If this thickness is small compared to the local dimensions of a satellite, such one-dimensional calculations are probably fairly accurate. Another requirement for steady-state theory to be valid is that

$$t_t R(t) \ll 1 . \quad (10)$$

This inequality just requires electron transit times to be short compared to other times of interest.

Figure 2 shows  $x_{\max}$  as a function of emission current density. It is apparent that the boundary layer can become quite thin as emission current goes up.

A more useful steady-state calculation would include realistic estimates of the actual electron energy and angular distributions created by low energy photoemission.

The electron distribution due to low energy photoemission is fairly well approximated by<sup>3,4</sup>

$$F(w, \theta, \phi) = \frac{1}{\pi} G(w) \sin\theta \cos\theta , \quad (11)$$

where  $G(w)$  is the electron energy distribution at emission,  $w$  is the electron energy, and  $\theta$  is the polar angle measured from the surface normal.

Note that the presence of an angular distribution complicates even a one-dimensional, monoenergetic approximation. Because one must project the velocity vector along the surface normal, a distribution of velocities along the surface normal appear even though the length of the velocity vector is constant.

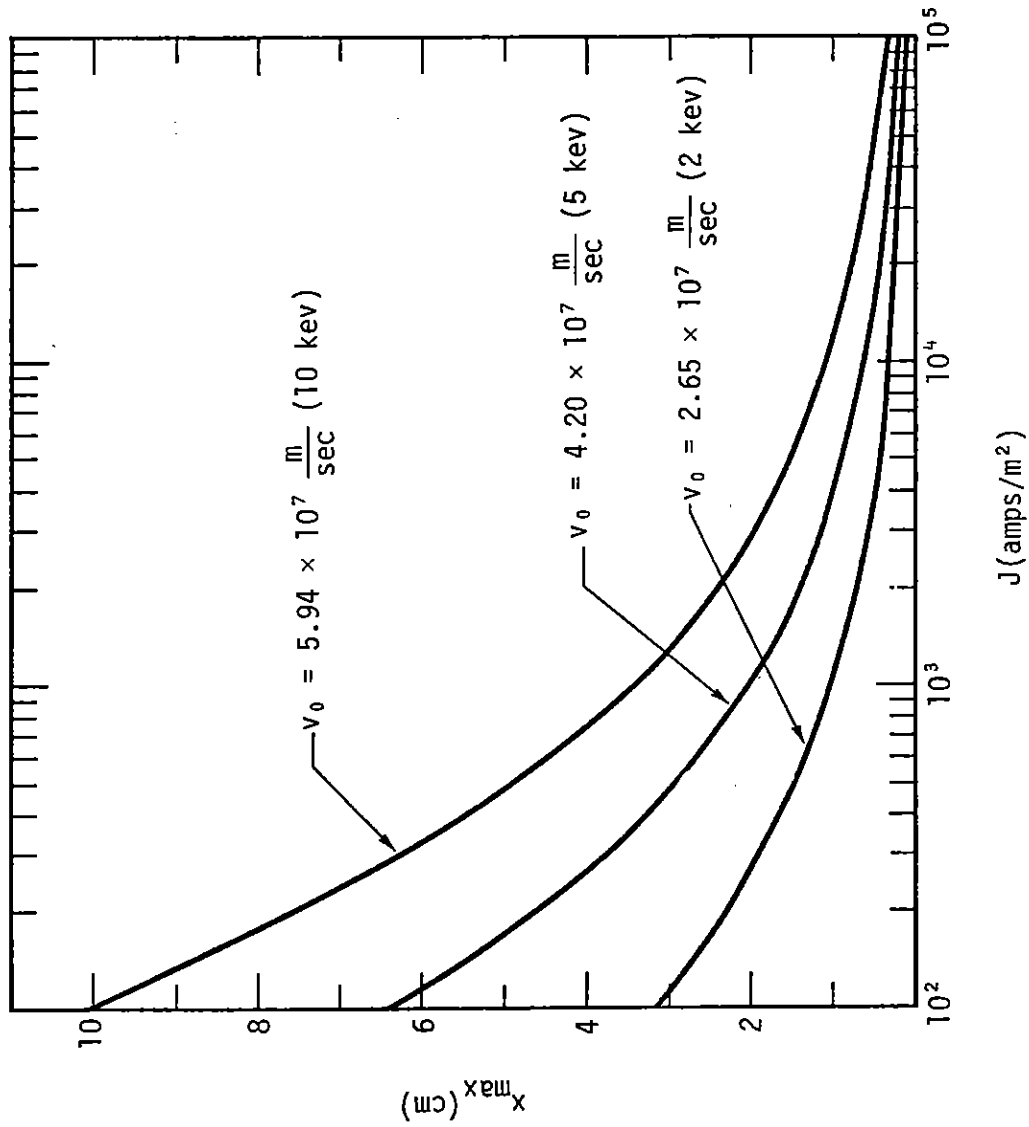


Figure 2. Boundary layer thickness,  $x_{\max}$ , as a function of emission current density,  $J$ —steady state approximation (Equation 9).

If the electron emission distribution shown in Equation 11 is assumed, then the projected phase space density is (see Appendix C)

$$f_1(x, w_x) = 2m \int_{w_x - e\phi}^{\infty} \frac{G(w)}{w} dw . \quad (12)$$

In this case, the surface normal is along the x-axis and

$$f_1(x, v_x) \equiv \iint f(\vec{v}) dv_y dv_z , \quad (13)$$

where  $f(\vec{v})$  is a solution of the Boltzmann equation. Also,

$$w_x = \frac{1}{2} m v_x^2 , \quad (14)$$

and  $\phi$  is the potential. The potential is assumed to be zero at the emission surface,  $x = 0$ .

Equation 12 is derived by setting the electron fluence at  $x = 0$  equal to twice the emission fluence as determined from Equation 11. The factor of two comes about since we assume a steady-state case with the number of electrons returning being equal to the number emitted.

The potential,  $\phi$ , is given by Poisson's equation

$$\frac{d^2\phi}{dx^2} = \frac{e}{\epsilon_0} N(x) , \quad (15)$$

where  $N(x)$  is the spatial electron density. Now

$$N(x) = \int_0^{\infty} f(x, w_x) dv_x , \quad (16)$$

which, using the steady-state value of  $f_1$ , is given by

$$N(x) = 2\sqrt{\frac{m}{2}} \int_0^{\infty} \frac{dw_x}{\sqrt{w_x}} \int_{w_x + V}^{\infty} \frac{G(w)}{w} dw , \quad (17)$$

where

$$V = -e\phi.$$

Note that  $N(x)$  depends on  $x$  only through  $V$ , so that  $N(x) \equiv N(V)$ , and by interchanging the order of integration, it can be shown that

$$N(V) = 4\sqrt{\frac{m}{2}} \int_V^\infty \frac{G(w) \sqrt{w-V}}{w} dw. \quad (18)$$

For convenience, define

$$N_0 \equiv N(V=0) = 4\sqrt{\frac{m}{2}} \int_0^\infty \frac{G(w)}{\sqrt{w}} dw, \quad (19)$$

and

$$\eta(V) = \frac{N(V)}{N_0}. \quad (20)$$

Then, Poisson's equation (Equation 15) can be written as

$$\frac{d^2V}{dx^2} = -\frac{e^2}{\epsilon_0} N_0 \eta(V). \quad (21)$$

If  $V$  is also normalized to some energy  $V_0$ , then Equation 21 can be written as

$$\frac{d^2\psi}{d\xi^2} = -\eta(\psi), \quad (22)$$

where

$$\psi = \frac{V}{V_0}. \quad (23)$$

$$\xi = \frac{x}{\lambda}, \quad (24)$$

and

$$\lambda = \sqrt{\frac{V_0 \epsilon_0}{N_0 e^2}}. \quad (25)$$

Since

$$\frac{\partial^2 \psi}{\partial \xi^2} = \frac{\partial}{\partial \psi} \left[ \frac{1}{2} \left( \frac{\partial \psi}{\partial \xi} \right)^2 \right], \quad (26)$$

it can be shown that

$$\frac{1}{2} \left( \frac{\partial \psi}{\partial \xi} \right)^2 = \mathcal{M}(\psi) + C_1, \quad (27)$$

where

$$\mathcal{M}(\psi) = \int_0^\psi \eta(\psi') d\psi', \quad (28)$$

and  $C_1$  is the integration constant

$$C_1 = \frac{1}{2} \left( \frac{\partial \psi}{\partial \xi} \right)^2 \Big|_{\xi=0}. \quad (29)$$

Now, the expression for  $\mathcal{M}(\psi)$  can be written as

$$\begin{aligned} \mathcal{M}(\psi) &= \int_0^\psi \left[ \frac{2\sqrt{2m}}{N_0} \int_{\psi'}^\infty \frac{G(w) \sqrt{w - \psi'}}{w} dw \right] d\psi' \\ &= \frac{2\sqrt{2m}}{N_0} \int_0^\infty dw \int_0^{\text{sm}(w, \psi)} \frac{G(w)}{w} \sqrt{w - \psi'} d\psi' \end{aligned} \quad (30)$$

where  $\text{sm}(w, \psi)$  means "the smaller of  $w$  and  $\psi$ " and  $w$  is also normalized to  $v_0$ . This expression can be reduced to

$$\begin{aligned} \mathcal{M}(\psi) &= \frac{4}{3} \frac{\sqrt{2m}}{N_0} \left\{ \int_0^\infty G(w) \sqrt{w} dw \right. \\ &\quad \left. - \int_\psi^\infty \frac{G(w)}{w} (w - \psi)^{3/2} dw \right\}. \end{aligned} \quad (31)$$



Also, Equation 27 can be used to obtain the expression

$$d\xi = \frac{d\psi}{\sqrt{2[C_1 - \mathcal{U}(\psi)]}}, \quad (32)$$

so that

$$\xi(\psi) = \int_0^\psi \frac{d\psi'}{\sqrt{2[C_1 - \mathcal{U}(\psi')]}}. \quad (33)$$

Equations 31 and 33 give the relationship between the normalized distance and voltage parameters for an arbitrary electron emission energy distribution,  $G(w)$ . The integrals in Equation 31 are first evaluated, either numerically or analytically, to determine  $\mathcal{U}(\psi)$ . It can be seen from Equation 27 that  $\mathcal{U}(\psi)$  is related to the square of the electric field.

The constant  $C_1$  is determined by Equation 29 or, if the electron energy distribution has a maximum electron energy,  $w_{\max}$ , then

$$C_1 = \mathcal{U}(\psi_{\max}), \quad (34)$$

where  $\psi_{\max}$  is the normalized potential corresponding to  $w_{\max}$ .

## SECTION 4

### FINITE DIFFERENCE CALCULATIONS

Finite difference techniques<sup>5-7</sup> have also been used to calculate SGEMP response and space charge limiting effects. A finite difference calculation divides the space outside the emission surface into a number of cells. The field or potential in each cell is assumed constant. Electrons moving in space are represented by particles whose trajectories are calculated using Newton's law. The position and velocity of these particles are then used as sources for the finite difference equivalent of Maxwell's equations. Thus, fields or voltages, and particle velocities and positions are calculated in a time-stepping procedure.

For a one-dimensional problem, this procedure is relatively easy to set up and run on the computer. The surface electric field from such a one-dimensional finite difference code is shown in Figure 3, along with plots of the early-time and steady-state approximations. For these calculations, monoenergetic 20 keV electrons were assumed to be emitted parallel to the surface normal vector. Figure 3 shows good agreement between the finite-difference calculation and the early-time approximation up to the time  $t_1$  when electrons first start returning. At later times, the finite difference code has an oscillatory behavior, the average of which is fairly well predicted by the steady-state approximation. This oscillatory behavior has been discussed by Birdsall and Bridges<sup>8</sup> and others. This instability is quite evident whenever monoenergetic energy spectra are assumed.

Thus far, only one-dimensional calculations have been considered. Such one-dimensional approximations are quite useful for providing a general

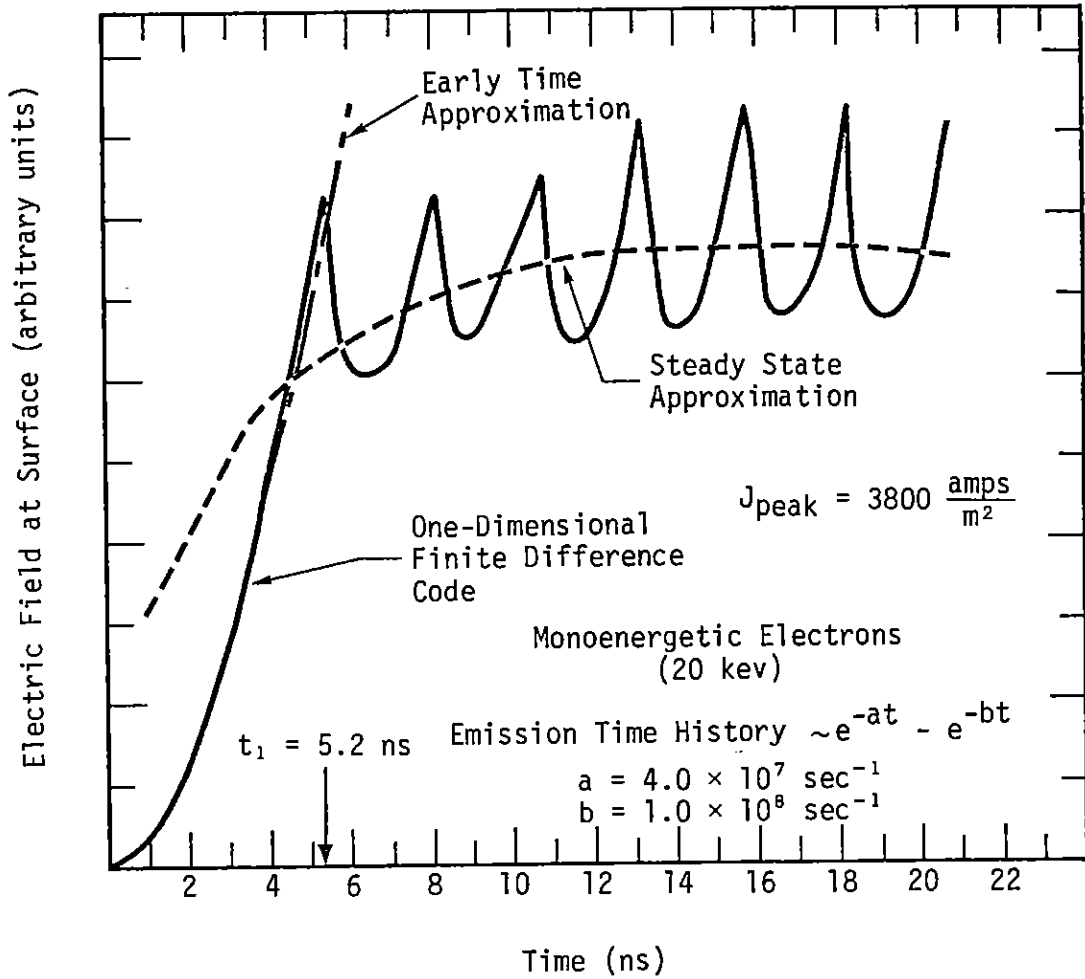


Figure 3. Comparison of early time approximation, steady state approximation, and finite difference calculation of surface electric field (one-dimensional planar geometry). ( $J_{\text{peak}}$  is the peak emission current, before space charge limiting, and  $t_1$  is the calculated time that electrons first start returning.)

understanding of the high space charge limited problem and application of one-dimensional theory is valid when considering distance scales small compared to any characteristic lengths of the system with which incident X rays are interacting.

However, finite difference techniques can, at least, conceptually, easily be extended to two or three dimensions and several 2-D, azimuthally symmetric SGEMP codes are now in existence. Such two-dimensional calculations point out several important effects that are lacking in any one-dimensional theory.

The most important difference between 1-D and 2-D calculations is that one-dimensional theory allows only longitudinal field components (longitudinal meaning along the emission surface normal) while two-dimensional results have both longitudinal and transverse components. An important result of allowing transverse components is that in 2-D calculations, a magnetic field will appear and skin currents will thus flow to replace emitted electrons. These replacement currents are an important first step in the overall coupling process from incident X rays to internal electronics.

Multi-dimensional finite difference calculations have a practical disadvantage, however. Two- or three-dimensional calculations require increasing amounts of computer time and storage as the number of grid cells and particles being tracked increases. Under conditions of high space charge limiting, spatial volumes near emission surfaces must be finely subdivided due to the steep longitudinal field gradients and many particles must be tracked inside this region. However, the rest of the space surrounding the test object must also be gridded, perhaps with larger cells, and some electrons will have sufficient energies to move significant distances away from emission surfaces. These requirements may result in very time-consuming and expensive computer runs.

## SECTION 5

### BOUNDARY LAYER TREATMENT

One method of avoiding the finite difference requirement of a very fine mesh near emission surfaces when a high degree of space charge limiting occurs is to combine a one-dimensional analytic approximation with the finite difference technique. In effect, such a hybrid method creates a "boundary layer" within the cells adjacent to emission surfaces. Some electrons are pulled back so rapidly by space charge limiting effects that they never leave the cell into which they are first emitted. These electrons are assumed trapped inside a boundary layer. Other electrons will escape through the boundary layer after having lost some part of their initial kinetic energy. These electrons can then be treated as in any finite difference, particle-following code. Thus, the boundary layer treatment serves as a way of subdividing the finite difference cell closest to the emission surface.

For a more detailed explanation, consider Figure 4. This figure shows a section of a finite difference mesh containing an emission surface. A two-dimensional azimuthally symmetric mesh is assumed and the field components are calculated at points where Maxwell's equations are automatically centered. The emission surface is assumed to be perfectly conducting and the boundary condition of zero tangential electric field is satisfied by placing the emission surface so that it passes through the  $E_r$  mesh points and setting the field at these mesh points equal to zero. The normal component of electric field,  $E_z$ , is then calculated at the points indicated by  $x$ , which are actually a distance of  $\Delta z/2$  from the emission surface.

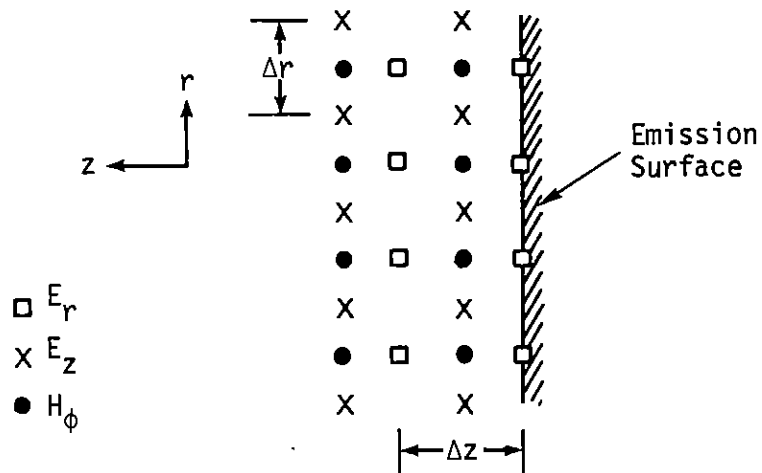


Figure 4. 2-D finite difference mesh.

If space charge limiting causes an electric field gradient varying significantly over one mesh cell ( $\Delta z$ ), then either the mesh size must be decreased or a boundary layer treatment can be used within the first cell of the mesh. In any case, it is assumed that the mesh is already small compared to any curvature of the emission surface; otherwise, the finite difference calculation would not be valid.

One way of integrating a boundary layer treatment into a finite-difference code is to use the steady-state, one-dimensional theory outlined in Section 3 of this report. The method presented here, however, differs in several ways from the ideal case discussed in Section 3. First of all, the factor of two in Equation 12 is not quite correct, since not all of the emitted electrons will be returning to the surface where they were emitted.

However, the very numerous low-energy electrons will be pulled back once space charge limiting effects become important and the actual factor in Equation 12 is probably only slightly less than two. Secondly, the boundary condition to the problem is now the normal electric field,  $E_z$ , at a distance  $\Delta z/2$  from the emission surface. It is required that the slope of the potential function, as calculated by steady state-theory, match the electric field at this grid point, as calculated by the finite-difference calculation.

In our sample grid (Figure 4), let  $\Delta z/2 = d$ . Then, from Equations 23-25, 27, and 33

$$\xi_d \equiv \frac{d}{\lambda} = \int_0^{\psi_d} \frac{d\psi'}{\sqrt{2[C_1 - \mathcal{H}(\psi')]}} , \quad (35)$$

and

$$\left. \frac{d\psi}{d\xi} \right|_{z=d} = - \frac{e\lambda}{V_0} \left. \frac{d\phi}{dz} \right|_{z=d} = \frac{e\lambda}{V_0} E_{z=d} , \quad (36)$$

so that

$$\begin{aligned} C_1 &= \frac{1}{2} \left( \left. \frac{\partial\psi}{\partial\xi} \right|_{\xi_d} \right)^2 + \mathcal{H}(\psi_d) \\ &= \frac{e^2\lambda^2}{2V_0} E_{z=d}^2 + \mathcal{H}(\psi_d) , \end{aligned} \quad (37)$$

where Equation 31 defines  $\mathcal{H}(\psi_d)$  as

$$\begin{aligned} \mathcal{H}(\psi_d) &= \frac{4}{3} \frac{\sqrt{2m}}{N_0} \left\{ \int_0^\infty G(w) \sqrt{w} dw \right. \\ &\quad \left. - \int_{\psi_d}^\infty \frac{G(w)}{w} (w - \psi_d)^{3/2} dw \right\} . \end{aligned} \quad (38)$$

Now, the basic inputs are the distance  $d$ , the electric field  $E_z(z=d)$ , and  $\mathcal{M}(\psi)$ , which is a function calculated from the emitted electron energy distribution,  $G(w)$ . The problem is to solve Equations 35 and 37 for  $\psi_d$ , the normalized potential. In general,  $\mathcal{M}(\psi)$  is a numerical rather than an analytic function and  $\psi_d$  can be found by some numerical iteration scheme.

$\psi_d$  is the normalized potential across the boundary layer. This potential defines the minimum energy required for an emitted electron to travel across the boundary layer (i.e., the first cell of the grid). Thus for the particle-following part of the finite difference code one can ignore all those electrons in the emission distribution having energy less than this minimum. Also, the initial energy of those electrons penetrating the boundary layer must be reduced by this same minimum energy.

This boundary layer treatment thus simplifies the electron following problem by indicating which electrons will "make it through" the boundary layer and into other cells of the finite difference mesh. The boundary layer may also have some direct effect on the external fields. A little thought shows that this can be true only if the boundary layer is not fully one-dimensional; i.e., a potential gradient parallel to the emission surface is required.

The boundary layer calculation gives a potential  $\phi_d$  at each  $E_z$  mesh point (see Figure 4) at each time step. The gradient of  $\phi_d$  along the  $\hat{r}$  direction is then just the tangential electric field created by the boundary layer. The electric field of the boundary layer can then be included in the finite difference calculation by setting  $E_r$  along the emission surface equal to this gradient ( $E_r$  would equal zero at all times for a perfect conductor without any boundary layer treatment).



## SECTION 6

### SUMMARY

This report reviews various approximations used for calculating the SGEMP response of an object under highly space-charge limited conditions. An early time approximation is used to calculate when space-charge limiting begins to become important. Steady-state calculations are then considered and a theory for realistic emission electron angular distributions and arbitrary energy distributions is developed. Finite difference calculations are then reviewed briefly. Finally, the combination of a one-dimensional, steady-state boundary layer calculation with a finite difference code is discussed. The use of this boundary layer treatment is shown to help avoid the requirement for very fine zoning of finite difference meshes near emission surfaces in cases of high space-charge limiting.

## REFERENCES

1. Karzas, W. J., and R. Latter, "Electromagnetic Radiation from a Nuclear Explosion in Space," Physical Review, 126, pp. 1919-1926, June 1962.
2. Hale, C. R., Electric Fields Produced by an Electronic Current Emitted Perpendicular to a Surface, Air Force Weapons Laboratory, Theoretical Note TN-115, April 1971.
3. Schaefer, R. R., "Simple Model of Soft X-ray Photoemission," J. Appl. Phys., Vol. 44, No. 1, January 1973.
4. Higgins, D. F., X-ray Induced Photoelectric Currents, Air Force Weapons Laboratory, Theoretical Note TN-178, June 1973.
5. Lopez, O., and W. F. Rich, IEEE Tran. Nucl. Sci., NS-20, No. 6, pp. 14-19, 1973.
6. dePlomb, E. P., and A. J. Woods, TEDIUM-RZ and RQ: Two-Dimensional Time-Dependent IEMP Computer Codes, Intelcom Rad Tech, DNA 3140F, March 1973.
7. Stettner, R., and D. F. Higgins, X-ray Induced Currents on the Surface of a Metallic Sphere, Mission Research Corporation, MRC-N-111, DNA 3612T, September 1974.
8. Birdsall, C. K., and W. R. Bridges, "Space-Charge Instabilities in Electron Diodes and Plasma Converters," Journal of Applied Physics, 32, pp. 2611-2617, December 1961.

APPENDIX A  
EARLY-TIME NON-SCREENING APPROXIMATION  
(Adapted from Ref. 1)

Since

$$\ddot{x} = - \frac{eE}{m} , \tag{A-1}$$

and the initial electron velocity is  $v_0$ , then

$$\dot{x} = 0 , \tag{A-2}$$

when

$$t = \frac{mv_0}{eE} . \tag{A-3}$$

The "turn-around time" for an electron moving in a constant field is then just

$$\begin{aligned} t_t &= \frac{2mv_0}{eE} \\ &= \frac{2mv_0}{\frac{eY}{\epsilon_0} \int_0^t R(t') dt'} , \end{aligned} \tag{A-4}$$

using Equation 1 for the electric field.

For a triangular pulse,

$$N(t) \equiv \int_0^t R(t') dt' = \frac{1}{2} \frac{t^2}{T^2} \text{ for } 0 < t < T . \tag{A-5}$$

Therefore,

$$t_t(t_e) \approx \frac{2mv_0\epsilon_0}{e^2YN(t_e)}, \quad (\text{A-6})$$

where  $t_e$  is the emission time of the electron being considered. By minimizing  $t_t$  with respect to  $t_e$  one can solve for  $t_0$ , the time when the first returning electron was emitted. If  $t_r$  is the return time,

$$t_t \equiv t_r - t_e. \quad (\text{A-7})$$

Then

$$t_r(t_e) = t_e + \frac{2mv_0\epsilon_0}{e^2N(t_e)Y}, \quad (\text{A-8})$$

and

$$\frac{dt_r(t_e)}{dt_e} = 1 + \frac{2mv_0\epsilon_0}{e^2Y} \frac{d}{dt_e} \left[ \frac{1}{N(t_e)} \right]. \quad (\text{A-9})$$

One minimizes the return time,  $t_r$ , by setting the derivative on the left-hand side of Equation A-9 equal to zero. Then

$$\left. \frac{d}{dt_e} N(t_e) \right|_{t_e=t_0} = \frac{e^2YN^2(t_0)}{2mv_0\epsilon_0}, \quad (\text{A-10})$$

but

$$\left. \frac{d}{dt_e} N(t_e) \right|_{t_e=t_0} \equiv G(t_0). \quad (\text{A-11})$$

Assuming  $t_0 < T$ , then

$$\frac{e^2Y}{2mv_0\epsilon_0} \left( \frac{1}{2} \frac{t_0^2}{T^2} \right)^2 = \frac{t_0}{T^2}, \quad (\text{A-12})$$

or, solving for  $t_0$ ,

$$t_0 = 2 \left[ \frac{mv_0\epsilon_0 T^2}{e^2Y} \right]^{1/3}. \quad (\text{A-13})$$

In this approximation, then, the turn-around-time is just

$$\begin{aligned}
 t_t &= t_1 - t_0 = \frac{2mv_0\epsilon_0}{e^2YN(t_0)} \\
 &= \left[ \frac{m\epsilon_0}{e^2} \frac{v_0T^2}{Y} \right]^{1/3}.
 \end{aligned} \tag{A-14}$$

The first returning electron then returns at

$$\begin{aligned}
 t_1 &= t_0 + t_t \\
 &= 3 \left[ \frac{m\epsilon_0}{e^2} \right]^{1/3} \left[ \frac{v_0T^2}{Y} \right]^{1/3}.
 \end{aligned} \tag{A-15}$$

Note that if  $t > T$ , the entire calculation is not valid due to the assumption used in obtaining Equation A-12.

The maximum distance from the emission surface reached by the first returning electron is then given by

$$\begin{aligned}
 x_{\max} &= \frac{mv_0^2}{2eE} = \frac{mv_0^2\epsilon_0}{2e^2YN(t_0)} \\
 &= \frac{v_0}{4} \left( \frac{m\epsilon_0}{e^2} \right)^{1/3} \left( \frac{v_0T^2}{Y} \right)^{1/3}.
 \end{aligned} \tag{A-16}$$



APPENDIX B  
STEADY STATE

From Poisson's equation

$$\frac{dE(x)}{dx} = - \frac{\rho(x)}{\epsilon_0} , \quad (B-1)$$

but for the steady state case

$$\rho(x) = \frac{2eYR(t)}{v(x)} . \quad (B-2)$$

Since

$$\ddot{x} = v(x) \frac{dv(x)}{dx} = - \frac{e}{m} E(x) , \quad (B-3)$$

then

$$\frac{d\ddot{x}}{dx} = \left( \frac{dv}{dx} \right)^2 + v(x) \frac{d^2v(x)}{dx^2} = - \frac{e}{m} \frac{dE(x)}{dx} , \quad (B-4)$$

which implies that

$$\frac{d^2}{dx^2} (v^2(x)) = \frac{4e^2YR(t)}{m\epsilon_0v(x)} . \quad (B-5)$$

This differential equation has the solution that

$$v(x) = [v_0^{3/2} - 3\sqrt{A}x]^{2/3} , \quad (B-6)$$

where

$$A = \frac{YR(t)e^2}{m\epsilon_0} = \frac{eJ(t)}{m\epsilon_0} , \quad (B-7)$$

where  $J(t)$  is the emission current density at time  $t$ .

One can also show by integration of Equation B-6 that

$$x = (3\sqrt{A})^{-1} [v_0^{3/2} - (v_0^{1/2} - \sqrt{A}t)^3], \quad (\text{B-8})$$

which gives the time between emission and return,  $t_t$ , as

$$t_t = 2 \left( \frac{v_0}{A} \right)^{1/2}. \quad (\text{B-9})$$

Also, the maximum distance an electron moves,  $x_{\max}$ , is found to be

$$x_{\max} = \frac{v_0^{3/2}}{3\sqrt{A}}. \quad (\text{B-10})$$

The total number of electrons outside the emitting surface is then given approximately by

$$N_{ss} \approx YG(t) t_t, \quad (\text{B-11})$$

and the electric field at the emission surface is

$$E_{ss}(x=0) = \frac{eN_{ss}}{\epsilon_0}. \quad (\text{B-12})$$



## APPENDIX C

### RELATION BETWEEN EMISSION SPECTRUM AND PHASE SPACE DENSITY

Assume that electrons are emitted from a planar surface located along the  $yz$ -plane of a Cartesian coordinate system. The phase space distribution function,  $f$ , then satisfies the time-independent Boltzmann equation

$$v_x \frac{\partial f}{\partial x} - \frac{eE}{m} \frac{\partial f}{\partial v_x} = 0, \quad (\text{C-1})$$

where it has been assumed that the only force acting on the emitted electrons is the electric field,  $E$ . The electron charge is designated by  $-e$  and the electron mass by  $m$ .

The phase space distribution function,  $f$ , is a function of  $x$ ,  $v_x$ ,  $v_y$ , and  $v_z$  and the electron flux density is

$$\text{flux density} = v_x f(x, v_x, v_y, v_z) = v_x f(x, \vec{v}). \quad (\text{C-2})$$

One now wants to relate  $f(x, \vec{v})$  to the electron emission spectrum at the planar surface under consideration. If this emission spectrum is written as  $F(w, \theta, \phi)$ , where  $w$  is the initial kinetic energy of the electron and  $\theta$  and  $\phi$  define the initial direction with respect to the surface normal, then

$$v_x f(x, \vec{v}) dv_x dv_y dv_z = F(w, \theta, \phi) dw d\theta d\phi. \quad (\text{C-3})$$

However,

$$dv_x dv_y dv_z = v^2 dv \sin\theta d\theta d\phi, \quad (\text{C-4})$$

and

$$dw = mv dv . \quad (C-5)$$

Therefore,

$$f(x=0, \vec{v}) = \frac{mF(w, \theta, \phi)}{v_x v \sin \theta} , \quad (C-6)$$

where  $x = 0$  since the phase space density is being equated to the electron emission distribution at the surface.

Now, if the emitted electrons are due to incident low-energy photons, the electron distribution is well approximated by

$$F(w, \theta, \phi) = \frac{1}{\pi} G(w) \sin \theta \cos \theta , \quad (C-7)$$

where  $G(w)$  is the electron energy distribution at emission.  $G(w)$  is a function of the emitting material and the incident photon spectrum. The angular distribution is measured with respect to the surface normal.

Combining Equations C-6 and C-7 gives

$$f(x=0, \vec{v}) = \frac{m}{\pi} \frac{G(w)}{v^2} . \quad (C-8)$$

Now define a new distribution function

$$f_1(v_x) \equiv \iiint f(\vec{v}) dv_y dv_z . \quad (C-9)$$

This distribution function is simply a projection of  $f(\vec{v})$  along the x-axis. If the kinetic energy is broken down into components parallel and perpendicular to the x-axis, then

$$w = w_x + w_{\perp} , \quad (C-10)$$

where

$$w_x = \frac{1}{2} m v_x^2 , \quad (C-11)$$

and

$$w_{\perp} = \frac{1}{2} m(v_y^2 + v_z^2) = \frac{1}{2} m v_{\perp}^2 . \quad (C-12)$$

Thus

$$\begin{aligned} f_1(v_x) &= \frac{m}{\pi} \iint \frac{G(w)}{v_x^2 + v_y^2 + v_z^2} dv_y dv_z \\ &= \frac{m}{\pi} \int \frac{G(w)}{v_x^2 + v_{\perp}^2} 2\pi v_{\perp} dv_{\perp} \\ &= m \int_{w_x}^{\infty} \frac{G(w)}{w} dw . \end{aligned} \quad (C-13)$$

This expression, then, gives the projected phase space distribution function at the surface as long as none of the emitted electrons are returning.

Now, it is a well known property of the Boltzmann equation that an arbitrary function of the constants of motion is a solution. Integrating Equation C-1 over the y- and z-components of velocity

$$v_x \frac{\partial f_1}{\partial x} - \frac{eE}{m} \frac{\partial f_1}{\partial v_x} = 0 . \quad (C-14)$$

Therefore,  $\mathcal{F}(w_x - e\phi)$ , where  $\mathcal{F}$  is an arbitrary function, is a solution of Equation C-14. In this case,  $\phi$  is the potential

$$\phi = - \frac{dE}{dx} . \quad (C-15)$$

Assuming  $\phi = 0$  at  $x = 0$ , Equation C-13 gives  $f_1(x=0, w_x)$  and  $f_1(x, w_x)$  is obtained by replacing  $w_x$  by  $w_x - e\phi$ ; i.e.,

$$f(x, w_x) = m \int_{w_x - e\phi}^{\infty} \frac{G(w)}{w} dw . \quad (C-16)$$

Note that this expression was obtained by assuming that the electron fluence at the emission surface was just equal to the emission fluence. This is true if none of the emitted electrons return to the emission surface (i.e., no space charge limiting). Another possibility is the steady-state situation, where electrons are returning to the surface at the same rate they are being emitted. For steady-state conditions, the value of  $f_1$  in Equation C-16 must be multiplied by a factor of 2 to account for those returning to the  $x = 0$  plane.